Molecular Cell, Vol. 4, 287–298, September, 1999, Copyright ©1999 by Cell Press

Mouse Lefty2 and Zebrafish Antivin Are Feedback Inhibitors of Nodal Signaling during Vertebrate Gastrulation

Chikara Meno,[1,8] Kira Gritsman,[4,8] Sachiko Ohishi,[2] Yasuhisa Ohfuji,[2] Elizabeth Heckscher,[4] Kyoko Mochida,[2] Akihiko Shimono,[3,7] Hisato Kondoh,[3] William S. Talbot,[4] Elizabeth J. Robertson,[5] Alexander F. Schier,[4,6] and Hiroshi Hamada[1,2,6]

[1]Division of Molecular Biology
Institute for Molecular and Cellular Biology
[2]CREST
Japan Science and Technology Corporation (JST)
[3]Division of Developmental Biology
Institute for Molecular and Cellular Biology
Osaka University
1-3 Yamada-oka
Suita, Osaka 565-0871
Japan
[4]Developmental Genetics Program
Skirball Institute of Biomolecular Medicine
Department of Cell Biology
NYU School of Medicine
New York, New York 10016
[5]Department of Molecular and Cellular Biology
Harvard University
Boston, Massachusetts 02115

Summary

Mammalian *lefty* and zebrafish *antivin* form a subgroup of the TGFβ superfamily. We report that mouse mutants for *lefty2* have an expanded primitive streak and form excess mesoderm, a phenotype opposite to that of mutants for the TGFβ gene *nodal*. Analogously, overexpression of Antivin or Lefty2 in zebrafish embryos blocks head and trunk mesoderm formation, a phenotype identical to that of mutants caused by loss of Nodal signaling. The *lefty2* mutant phenotype is partially suppressed by heterozygosity for *nodal*. Similarly, the effects of Antivin and Lefty2 can be suppressed by overexpression of the *nodal*-related genes *cyclops* and *squint* or the extracellular domain of ActRIIB. Expression of *antivin* is dependent on Nodal signaling, revealing a feedback loop wherein Nodal signals induce their antagonists Lefty2 and Antivin to restrict Nodal signaling during gastrulation.

Introduction

The vertebrate body plan is established during gastrulation when the three germ layers form and the embryonic axes are determined. Genetic analyses in mouse and zebrafish have revealed the essential role of the TGFβ-related signal Nodal in this process (Zhou et al., 1993; Conlon et al., 1994; Feldman et al., 1998). Mouse *nodal* mutants lack the primitive streak and show a severe reduction of mesoderm formation (Zhou et al., 1993; Conlon et al., 1994). Similarly, double mutants for the zebrafish nodal-related genes *squint* (*sqt*) and *cyclops* (*cyc*) are impaired in germ layer formation (Feldman et al., 1998; Rebagliati et al., 1998a; Sampath et al., 1998). In addition, Nodal signaling is involved in neural patterning (Hatta et al., 1991; Feldman et al., 1998; Rebagliati et al., 1998a; Sampath et al., 1998), anterior development (Varlet et al., 1997a), and left–right axis determination (Collignon et al., 1996; Lowe et al., 1996; Varlet et al., 1997b).

The Nodal signaling pathway has not been analyzed at the biochemical level, but genetic studies indicate that Nodal signals might act via Activin-like receptors (Oh and Li, 1997; Gu et al., 1998; Gritsman et al., 1999; reviewed in Harland and Gerhart, 1997; Massague, 1998). Additional complexity in Nodal signaling has recently been revealed by the finding that maternal-zygotic mutants for the zebrafish EGF-CFC gene *one-eyed pinhead* (Zhang et al., 1998) lack Nodal signaling and display a phenotype identical to *sqt;cyc* double mutants (Gritsman et al., 1999). These results indicate that Nodal signals not only require TGFβ-like receptors, but are also dependent on extracellular cofactors of the EGF-CFC family.

A novel family of TGFβ molecules implicated in vertebrate embryogenesis has recently been identified by the cloning of mouse *lefty1* and *lefty2* and zebrafish *antivin* (Meno et al., 1996, 1997; Thisse and Thisse, 1999). These proteins lack the long alpha helix involved in homodimerization and heterodimerization of TGFβ signals and lack a cysteine residue implicated in stabilizing these complexes. These structural considerations suggest that the Lefty-like proteins may function differently than other TGFβ family members. Notably, *lefty1, lefty2*, and *antivin* are expressed in patterns overlapping with *nodal*, *sqt*, and *cyc*. In mice, *nodal* is expressed throughout the epiblast and primitive endoderm at pregastrulation stages. Expression in the endoderm lineage is uniform and highly transient, and *nodal* expression overlaps briefly with that of *lefty1* in cells of the anterior visceral endoderm (AVE) at E6.5 before being downregulated. *lefty2* is expressed in nascent mesoderm arising in the mid-distal region of the streak at gastrulation, an expression domain that temporally coincides with downregulation of *nodal* in cells of the posterior epiblast fated to enter the streak (Varlet et al., 1997a; Oulad-Abdelghani et al., 1998; this study). Finally, at early somite stages, *nodal* and *lefty2* are coexpressed in the left lateral plate mesoderm. Similarly, zebrafish *antivin*, and *cyc* or *sqt* are coexpressed in mesodermal and endodermal precursors of the blastula margin, the axial midline, and the left lateral plate (Feldman et al., 1998; Rebagliati et al., 1998b; Sampath et al., 1998; Thisse and Thisse, 1999).

Analysis of *lefty1* mutants has established a role for this gene in left–right axis determination (Meno et al., 1998), but the role of the Lefty family in signaling has

[6]To whom correspondence should be addressed (e-mail: hamada@imcb.osaka-u.ac.jp [H. H.], schier@saturn.med.nyu.edu [A. F. S.]).
[7]Present address: Division of Cell Differentiation, National Institute for Basic Biology, Myodaiji-cho, Okazaki 444-8585, Japan.
[8]These authors contributed equally to this work.

remained unclear (reviewed in Beddington and Robertson, 1999). For instance, it has been proposed that Antivin, Lefty1, and Lefty2 antagonize signaling by TGFβ ligands such as Activin or BMPs (Meno et al., 1997; Thisse and Thisse, 1999). In addition, it has been suggested that Nodal and Lefty might act synergistically because Nodal, Lefty1, and Lefty2 can induce expression of the transcription factor Pitx2 in the chick lateral plate mesoderm (Logan et al., 1998; Piedra et al., 1998; Ryan et al., 1998; Yoshioka et al., 1998).

To learn more about the role of the Lefty family, we combined loss- and gain-of-function approaches in mouse and zebrafish. *lefty2* mutant mouse embryos showed an expansion of the primitive streak and excess formation of mesoderm, a phenotype opposite to that of *nodal* mutants. The *lefty2* mutant phenotype was partially suppressed by heterozygosity for *nodal*, suggesting antagonistic effects of the two proteins. In addition, we found that Lefty2 and Antivin act as antagonists of Nodal signaling in zebrafish and induce phenotypes identical to *sqt;cyc* and maternal-zygotic *oep* mutants. The effects of Antivin overexpression can be overcome by overexpression of Nodal signals or the extracellular domain of the type II activin receptor ActRIIB, suggesting that this receptor is a target of Antivin action. Finally, we found that expression of *antivin* is dependent on Nodal signaling, suggesting that Lefty2 and Antivin block Nodal signaling in a negative feedback mechanism, allowing tight control of Nodal signaling during vertebrate gastrulation.

Results

lefty2 Null Mutants Are Early Embryonic Lethal

The murine "*lefty*" locus is composed of two highly conserved genes, *lefty1* and *lefty2*, which are tightly linked on chromosome 1 (Meno et al., 1997). To examine the role of *lefty2* in gastrulation and L–R asymmetry, we generated mutant mice deficient in *lefty2*. To inactivate *lefty2*, we constructed a targeting vector that removes all four exons of *lefty2* after homologous recombination (Figure 1A). Two correctly targeted ES cells clones were used to generate *lefty2*$^{+/-}$ heterozygotes. Mutant embryos derived from both cell lines showed identical phenotypes (see below). *lefty2*$^{+/-}$ heterozygous mice were normal and fertile. When intercross progeny from *lefty2*$^{+/-}$ heterozygous mice were genotyped at birth, no homozygous animals were found, indicating that *lefty2* null mutants are embryonic lethal. To characterize the embryonic lethality, we initially analyzed litters from heterozygous intercrosses at embryonic days 8.0 (E8.0) to E11.5. At E8.25, homozygous mutant embryos were present at roughly the expected frequency of 25% but were morphologically abnormal. At E11.5, a significant number of embryos were being reabsorbed, all of which turned out to be homozygous mutants (Figure 1B). Thus, loss of Lefty2 activity leads to embryonic lethality before L–R defects can be analyzed. The early defects suggest that *lefty2* has important roles during the process of gastrulation, likely reflecting its earliest expression in mesoderm populations at E6.5 and E7.5 (Meno et al. 1997; Figures 1C–1F).

In situ hybridization confirmed the absence of *lefty2* mRNA in the mesoderm of homozygous mutant embryos (Figure 1K), establishing that the targeting event resulted in a null allele. Because *lefty1* and *lefty2* are tightly linked to each other on mouse chromosome 1, it was important to test whether the deletion of *lefty2* exons affected *lefty1* expression in *cis*. Normally, *lefty1* is transiently expressed in the anterior visceral endoderm (AVE) at E6.5 and E6.75 (Oulad-Abdelghani et al., 1998; Figures 1G and 1H), and expression is no longer detected at E7.0 (Figure 1I). In *lefty2* mutant embryos, *lefty1* was correctly expressed in the AVE at E6.75 (Figure 1K), confirming that the targeted deletion of *lefty2* exons did not affect *lefty1* expression in *cis*.

Expansion of the Primitive Streak and Excess Mesoderm Formation in *lefty2* Mutant Embryos

At E9.5, the embryonic region of homozygous mutants showed no signs of axial patterning and instead remained as a mass of cells lacking distinguished structure at the distal end (Figure 2C). The extraembryonic structures were less severely affected. Although the yalk sac was formed, blood vessels were not found, and the endodermal and mesodermal components of the yalk sac were dissociated. The allantois, derived from posterior mesoderm produced at the proximal end of the primitive streak, formed normally but failed to fuse appropriately to the chorion, likely due to the unusual topology of the mutant embryo (Figure 2C).

To determine the onset of morphological anomalies, we examined homozygous embryos at earlier stages. *lefty2*$^{-/-}$ embryos appeared morphologically and histologically normal until E7.5 (data not shown; also see Figure 7). At the early somite stage (E8.0-E8.25), the extraembryonic structures were relatively normal, and blood islands were seen in the yolk sac (Figures 2D–2H). The embryonic region, however, showed severe defects. The head folds, somites, heart, and notochord were absent (Figures 2D–2J). Instead, a mass of mesoderm-like cells accumulated in the posterior/distal region of the embryo proper and in the lateral region adjacent to the embryonic–extraembryonic junction. Histological observations indicated that the region of ingressing ectoderm was markedly expanded (Figures 2I and 2J), suggesting that the primitive streak was expanded laterally. In the anterior-distal region, an abnormal indentation or groove developed instead of the definitive node (Figure 2E, arrowhead).

Examination of various marker genes confirmed the morphological and histological observations described above (Figure 3). First, we examined *T* and *fgf8* as markers of nascent mesoderm demarcating the primitive streak (Kispert and Herrmann, 1994; Crossley and Martin, 1995). In wild-type and *lefty2* mutants at E7.75, *T* was expressed in the primitive streak and head process (Figure 3A). At E8.0, however, *T* expression was found to extend more laterally (Figures 3C and 3F). Moreover, the *T*-expressing domain in the midline failed to extend anteriorly (Figures 3C and 3D), suggesting that the notochord fails to form in *lefty2* mutant embryos. The domain of *fgf8*-expressing cells was similarly expanded (Figures 3I, 3J, and 3L). Collectively these results reveal that loss of Lefty2 activity results in a dramatic expansion of the

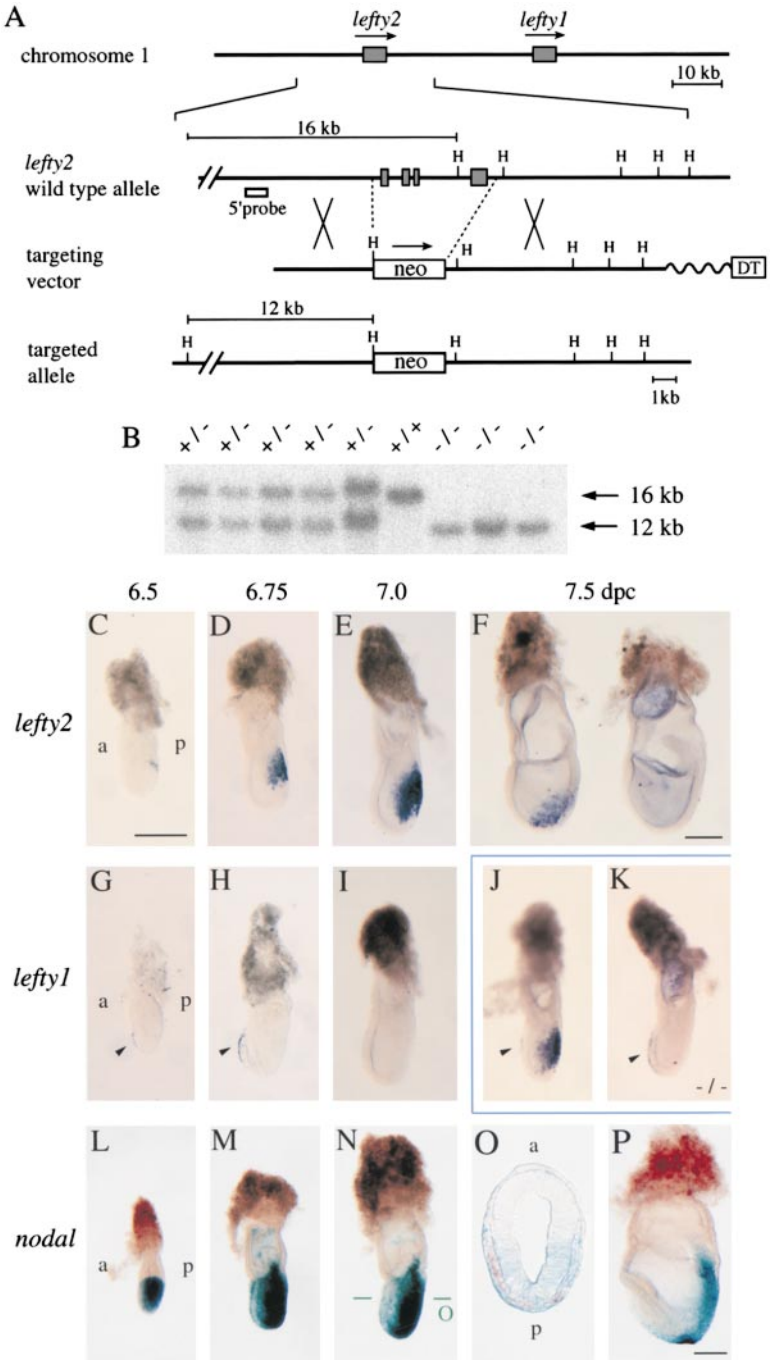

Figure 1. Generation of Mutant Mice Lacking *lefty2*

(A) The *lefty2* gene and targeting strategy. The relative positions of *lefty1* and *lefty2* on mouse chromosome 1 are shown at the top, with the direction of transcription indicated by arrows. H; Hind III. After homologous recombination, all the exons of *lefty2* (shaded boxes) are replaced by the *neo* gene. DT, diphtheria toxin A.

(B) Southern blot analysis of one litter of embryos at E11.5 that was obtained from the intercrossing of *lefty2*$^{+/-}$ heterozygotes. Genomic DNA was digested with HindIII and subjected to hybridization with the probe indicated in (A). Arrows indicate the 16 kb (wild-type) and 12 kb (mutant) fragments.

(C–I) Expression of *lefty1* and *lefty2* in wild-type embryos between E6.5 and E7.5. In the wild-type embryos, *lefty1* is expressed in the anterior visceral endoderm (arrowheads) between E6.5 and E6.75 (G and H) while *lefty2* is expressed in newly formed mesoderm between E6.5 and E7.5 (C–F). Both genes show asymmetric expression at E8.0–E8.25 (Meno et al., 1997).

(J and K) *lefty1* and *lefty2* mRNAs were simultaneously detected in the wild-type (J) and *lefty2* mutant (K) embryos with the probe that recognizes both *lefty1* and *lefty2*. In the *lefty2* mutant embryos (K), *lefty1* expression was present in the anterior visceral endoderm (arrowhead) while *lefty2* expression was absent. The anterior–posterior (a–p) axis is indicated.

(L–P) Expression of *nodal* in *nodal*$^{lacZ/+}$ embryos. *nodal* expression was visualized by X-gal staining. In (O), an X-gal-stained embryo shown in (N) was subjected to in situ hybridization with the *lefty2* probe. *nodal* expression (blue) is seen in the posterior ectoderm, nascent mesoderm, and endoderm whereas *lefty2* expression (red) is present in the newly formed mesoderm. At E7.75 (P), X-gal staining is mainly observed in the node. *nodal* expression in the ectoderm and endoderm has decreased. Scale bars represent 250 μm.

primitive streak leading to the formation of excess mesoderm, consistent with the histological observations (Figure 2J). Interestingly, this phenotype is in marked contrast to that of *nodal* null mutants, which are impaired in primitive streak formation and are, consequently, largely devoid of mesoderm (Conlon et al., 1994).

Further analysis of *lefty2* mutants indicated that the nascent mesoderm failed to migrate and become appropriately patterned at late gastrulation stage. For example, expression of *mox-1*, a marker for the paraxial mesoderm (Candia et al., 1992), was absent (Figure 3N). The expression of *twist*, a marker for the lateral plate mesoderm, paraxial mesoderm, head mesenchyme, and the allantois (Wolf et al., 1991), was abolished except in the allantois and a small population of distally accumulated mesoderm cells (Figure 3P). Interestingly, the accumulated mesoderm-like cells expressed *otx2*, a gene normally confined to anterior neuroectoderm (Ang et al., 1994), suggesting defects in cell-type specification or differentiation (Figure 3X). The expression of *HNF3*-β, a marker for axial midline structures such as notochord, floor plate, and definitive endoderm at early somite stages (Sasaki and Hogan, 1993), was absent except in the anterior region of the primitive streak and the indentation marking the distal tip of the expanded streak (Figure 3R). The expression of *Shh*, another marker for

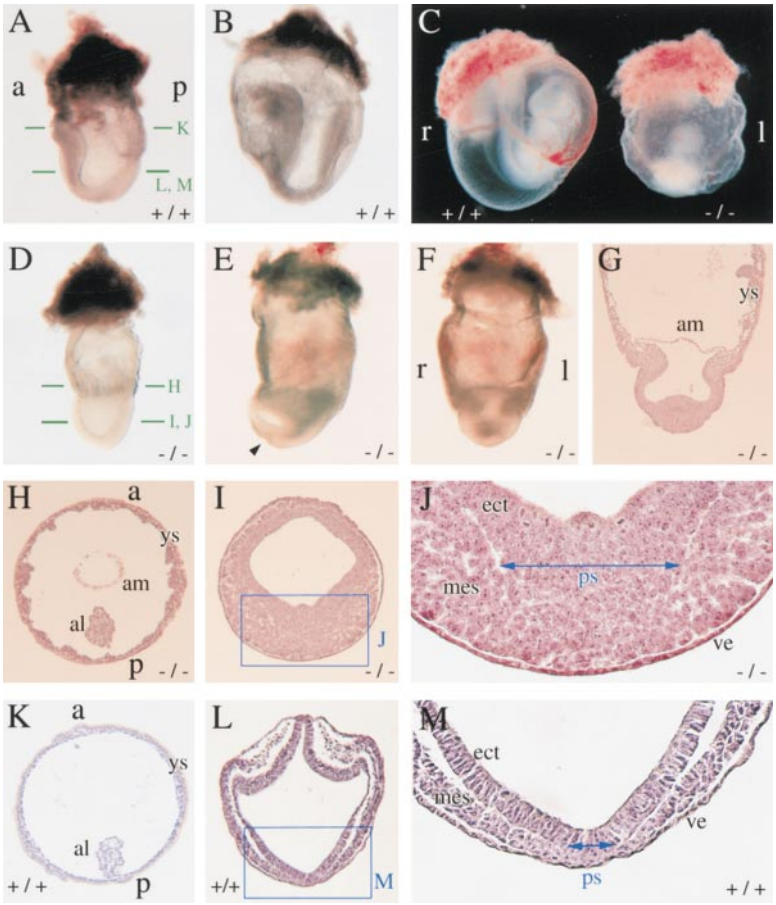

Figure 2. Morphology and Histology of *lefty2*$^{-/-}$ Embryos

(A–F) Whole-mount views of the wild-type (+/+) and *lefty2*$^{-/-}$ (−/−) embryos are shown. Lateral views are shown except for (C) and (F). (F) is an anterior view of the embryo shown in (E). Developmental stages are E8.0 in (A) and (D), E8.25 in (B), (E), and (F), and E9.5 in (C).

(G) A frontal section of the embryo shown in (E) and (F).

(H–J) Transverse sections of the mutant embryo shown in (D).

(K–M) Transverse sections of the wild-type embryo shown in (A). (J) and (M) are magnified views of the areas indicated in (I) and (L). The region of the ingressing ectoderm is indicated by the blue arrow (J), which is markedly expanded in the mutant embryo. al, allantois; am, amnion; ect, embryonic ectoderm; mes, embryonic mesoderm; ps, primitive streak; ve, visceral endoderm; ys, yolk sac.

axial structures, was absent except in a small anterior region of the midline (Figure 3T). *Hesx-1* expression marks the AVE at E6.5, and expression extends into the anterior neuroectoderm at E8.0 (Thomas and Beddington, 1996). In the mutant embryos, *Hesx-1* was found to be expressed appropriately in the AVE and then in the adjacent ectoderm (Figure 3V; data not shown), suggesting that formation of a functional AVE is unaffected in *lefty2* mutant embryos. These results show that *lefty2* is required for the correct specification of the mesoderm generated along the proximal-distal length of the streak during gastrulation. Consequently, *lefty2* mutant embryos fail to form organized structures such as the node, notochord, and somites. The anterior–posterior axis of the mutant embryo appears to be specified correctly, but distinct anterior structures such as the head folds do not form correctly.

nodal Heterozygosity Partially Rescues the *lefty2* Phenotype

Intriguingly, the expansion of the primitive streak in *lefty2* null mutant embryos is the opposite of the phenotype of *nodal* mutants, which fail to form a primitive streak (Conlon et al., 1994). This finding suggested the hypothesis that Nodal and Lefty2 might act antagonistically during mesoderm formation. To assess this possibility, we examined the potential genetic interaction between *lefty2* and *nodal* by crossing *lefty2* and *nodal*^{lacZ} mutants (Collignon et al., 1996). Double heterozygotes (*lefty2*$^{+/-}$ *nodal*$^{lacZ/+}$) appeared to be normal and were intercrossed to obtain embryos with various genotypic combinations. Embryos homozygous for the *nodal* mutation showed the same severe phenotype (the lack of primitive streak formation [Conlon et al., 1994]), regardless of the genotype of *lefty2* (data not shown). In particular, *lefty2*$^{-/-}$ *nodal*$^{lacZ/lacZ}$ embryos were identical to *lefty2*$^{+/+}$ *nodal*$^{lacZ/lacZ}$ embryos, establishing that the expansion of mesoderm in *lefty2* mutants is dependent on Nodal signaling. Strikingly, the defects of *lefty2*$^{-/-}$ *nodal*$^{lacZ/+}$ embryos were less severe than those of *lefty2*$^{-/-}$ *nodal*$^{+/+}$ mutants at E8.25 (Figure 4). Less excess mesoderm accumulated in *lefty2*$^{-/-}$ *nodal*$^{lacZ/+}$ embryos (Figure 4D), and the neural folds, which were absent in *lefty2*$^{-/-}$ *nodal*$^{+/+}$ embryos, were frequently present in the *lefty2*$^{-/-}$ *nodal*$^{lacZ/+}$ embryos (Figure 4D). The allantois, which was not connected to the chorion in *lefty2*$^{-/-}$ *nodal*$^{+/+}$ embryos (Figures 2C and 4A), was often correctly fused to the chorion in *lefty2*$^{-/-}$ *nodal*$^{lacZ/+}$ embryos (data not shown). In spite of this partial rescue, the *lefty2*$^{-/-}$ *nodal*$^{lacZ/+}$ embryos die at late gastrulation.

Partial rescue of the *lefty2* null phenotype by *nodal* heterozygosity was further confirmed with molecular markers (Figures 4E–4H). *T* expression, which was expanded laterally in the primitive streak and never extended to the anterior region of the midline in *lefty2* null mutants (Figures 3C, 3D, and 3F), did extend anteriorly and was less expanded laterally in *lefty2*$^{-/-}$ *nodal*$^{lacZ/+}$

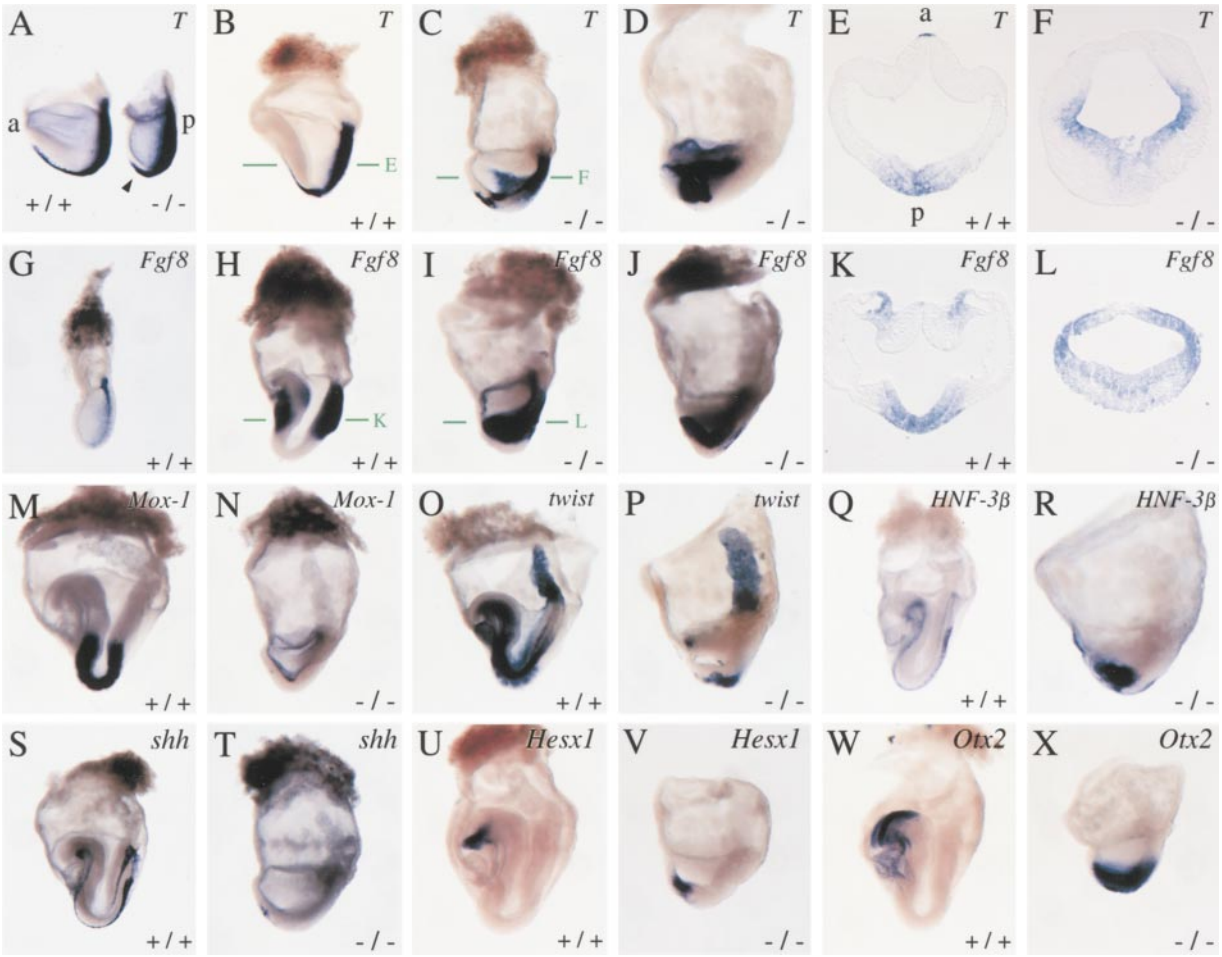

Figure 3. Aberrant Expression of Various Marker Genes in *lefty2* Mutant Embryos

Expression of various markers in wild-type (+/+) and *lefty2* mutant (−/−) embryos was examined by whole-mount in situ hybridization. Developmental stages are E7.75 (A), E7.5 (G), or E8.0–8.25 (B–F, H–X). The name of the probes and genotypes of embryos are indicated in each panel. Lateral views are shown. The embryos shown in (B), (C), (H), and (I) were sectioned after the hybridization, and transverse sections are shown in (E), (F), (K), and (L), respectively.

embryos (Figures 4E and 4G). Similarly, the expanded expression of *fgf8* was partially reduced in *lefty2*$^{-/-}$ *nodal*$^{lacZ/+}$ embryos (Figure 4H). The expression of *Shh*, which was almost abolished in *lefty2*$^{-/-}$ *nodal*$^{+/+}$ embryos (Figure 3T), was seen in the midline along the A–P axis (data not shown). These results reveal antagonistic genetic interactions between *lefty2* and *nodal* and suggest a role for Lefty2 as an inhibitor of Nodal signaling during formation of the mesodermal lineage.

Mouse Lefty2 and Zebrafish Antivin Inhibit Nodal Signaling in Zebrafish Embryos

The results described above provide evidence that Nodal and Lefty2 act antagonistically during mouse embryogenesis. To further study the regulation and evolutionary conservation of this interaction, we turned to zebrafish. Our recent studies have identified the *nodal*-related genes *cyc* and *sqt* and the EGF-CFC gene *oep* as essential components of Nodal signaling in zebrafish (Feldman et al., 1998; Zhang et al., 1998; Gritsman et al., 1999). We noted that overexpression of Lefty2 (Figure 5D), Lefty1, and zebrafish Antivin (Thisse and Thisse, 1999; Figure 5E) induces phenotypes that strongly resemble *sqt;cyc* double mutants (Feldman et al., 1998; Figure 5B) and maternal-zygotic *oep* mutants (Gritsman et al., 1999; Figure 5C). In particular, no head and trunk mesoderm and endoderm forms and gastrulation movements are severely impaired (Thisse and Thisse, 1999; data not shown). In addition, activation of Activin signaling appeared to suppress the effects of Antivin, leading to the suggestion that Antivin might be an antagonist of Activin (Thisse and Thisse, 1999). In light of our studies on zebrafish Nodal signaling and the *lefty2* mutant phenotype, we reasoned that Antivin might regulate the activity of Nodal signaling in zebrafish. We first tested this idea by determining if Antivin/Lefty2 and Sqt/Cyc act antagonistically. Overexpression of Antivin and Lefty2 inhibits the expression of the dorsal markers *goosecoid* and *sonic hedgehog* (Thisse and Thisse, 1999; Figures 5J and 5P; data not shown) whereas overexpression of Sqt or Cyc induces ectopic *goosecoid* and *hedgehog* expression (Toyama et al., 1995; Feldman et al., 1998; Rebagliati et al., 1998b; Gritsman et al., 1999; Figures 5K, 5M, 5Q, and 5S). Coexpression of Sqt

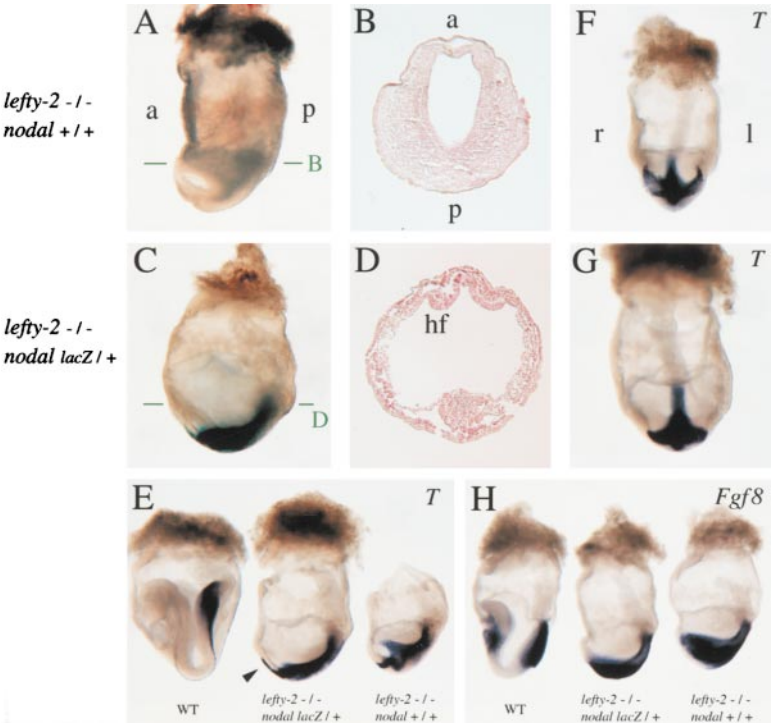

Figure 4. *nodal* Heterozygosity Suppresses the *lefty2* Phenotype

(A–D) E8.25 *lefty2*$^{-/-}$ embryos with (C and D) or without (A and B) a mutant *nodal* allele (*nodal lacZ*) are shown in comparison. (B) and (D) are the sections of the embryo shown in (A) and (C), respectively. The accumulation of mesoderm, which is apparent in (B), is not obvious in (D). The head fold (hf) is not formed in (B) but is formed in (D). Section in (D) was counterstained with nuclear fast red.

(E) *T* expression in wild-type (left), *lefty2*$^{-/-}$ *nodal*$^{lacZ/+}$ (middle), and *lefty2*$^{-/-}$ *nodal*$^{+/+}$ (right) embryos. Lateral views are shown. Anterior extension of axial *T* expression in the *lefty2*$^{-/-}$ *nodal*$^{lacZ/+}$ embryo is indicated by an arrowhead.

(F and G) *T* expression in the *lefty2*$^{-/-}$ *nodal*$^{+/+}$ (F) and *lefty2*$^{-/-}$ *nodal*$^{lacZ/+}$ (G) embryos. Anterior views show that the lateral expansion of *T* expression is less severe in the *lefty2*$^{-/-}$ *nodal*$^{lacZ/+}$ embryo (G).

(H) *fgf8* expression in wild-type (left), *lefty2*$^{-/-}$ *nodal*$^{lacZ/+}$ (middle), and *lefty2*$^{-/-}$ *nodal*$^{+/+}$ (right) embryos. The expansion of *fgf8* expression is less severe in the *lefty2*$^{-/-}$ *nodal*$^{lacZ/+}$ embryo.

or Cyc with Antivin or Lefty2 can overcome the effects of Antivin and Lefty2 and vice versa (Figures 5L, 5R, 5N, and 5T; data not shown). These results establish that Nodal/Sqt/Cyc and Lefty/Antivin act as agonist and antagonist, respectively, during early embryogenesis.

Previous studies have indicated that Cyc and Sqt activate and Antivin inhibits activin-like receptors (Gritsman et al., 1999; Thisse and Thisse, 1999). To further test this idea and determine in more detail how Nodal-related proteins and Antivin might antagonize each other, we coexpressed Sqt or Antivin with the extracellular domain of the type II activin receptor ActRIIB (Aexd; Dyson and Gurdon, 1997). Strikingly, the opposing phenotypic effects caused by Sqt (Figure 5G) or Antivin (Figure 5E) can both be completely blocked by the ActRIIB ectodomain (Figures 5F and 5H), suggesting that the ActRIIB receptor might be a common target of Sqt and Antivin.

Regulation of *antivin* by Nodal Signaling

antivin expression closely follows the expression of *cyc* and *sqt* (Feldman et al., 1998; Rebagliati et al., 1998b; Sampath et al., 1998; Thisse and Thisse, 1999; Figure 6). In particular, *antivin* is first expressed at the dorsal margin, similar to *sqt* (Figures 6A and 6D) and then in all marginal cells, similar to *sqt* and *cyc* (Figures 6F, 6I, 6N, 6P, and 6T). These observations suggested that *antivin* transcription might either be activated by Nodal signaling or might be initiated concomitantly with *cyc* and *sqt*. To determine the regulatory link between the transcription of *antivin* and the Nodal signaling pathway, we examined *antivin* expression in *sqt;cyc* double mutants and maternal-zygotic *oep* mutants, two mutant combinations that inactivate Nodal signaling (Feldman et al., 1998; Gritsman et al., 1999). We find that in the absence of Nodal signaling, *antivin* expression at the dorsal margin is initiated, but not maintained, whereas lateral and ventral expression is completely dependent on Nodal signaling (Figures 6E, 6J, and 6O, and data not shown). In contrast, expression of marginal markers such as *Brachyury/T* or *wnt11* is maintained in maternal-zygotic *oep* or *sqt;cyc* mutants (Feldman et al., 1998; Gritsman et al., 1999). In addition, overexpression of Nodal signals induces the widespread expression of *antivin* (Figure 6W; data not shown). These results establish that Nodal signaling initiates a negative feedback loop by activating the expression of the Nodal antagonist Antivin in most mesodermal and endodermal progenitors.

Antivin Blocks *nodal* Autoregulation

To determine if, similar to *antivin*, transcription of *cyc* and *sqt* is dependent on Nodal signaling, we analyzed the expression of these genes in maternal-zygotic *oep* mutants (Figure 6; data not shown). In contrast to *antivin* expression, we find that initial expression of *cyc* and *sqt* is independent of Nodal signaling (Figures 6C, 6H, and 6R). At later stages, however, Nodal signaling is required for maintenance of *cyc* and *sqt* expression (Figures 6M and 6V). These results reveal a positive feedback loop in which Nodal signaling maintains the expression of *cyc* and *sqt*.

The phenotypic effects induced by overexpression of Antivin or Lefty2 might be caused by blocking Nodal signaling and/or by blocking expression of *cyc* and *sqt*. To distinguish between these possibilities, we analyzed the expression of *cyc* and *sqt* in embryos that overexpress Lefty2 or Antivin. As was observed in maternal-zygotic *oep* mutants, overexpression of Antivin and Lefty2 blocked the maintenance, but not initiation, of *cyc* and *sqt* expression (Figures 6B, 6G, 6L, 6Q, and 6U;

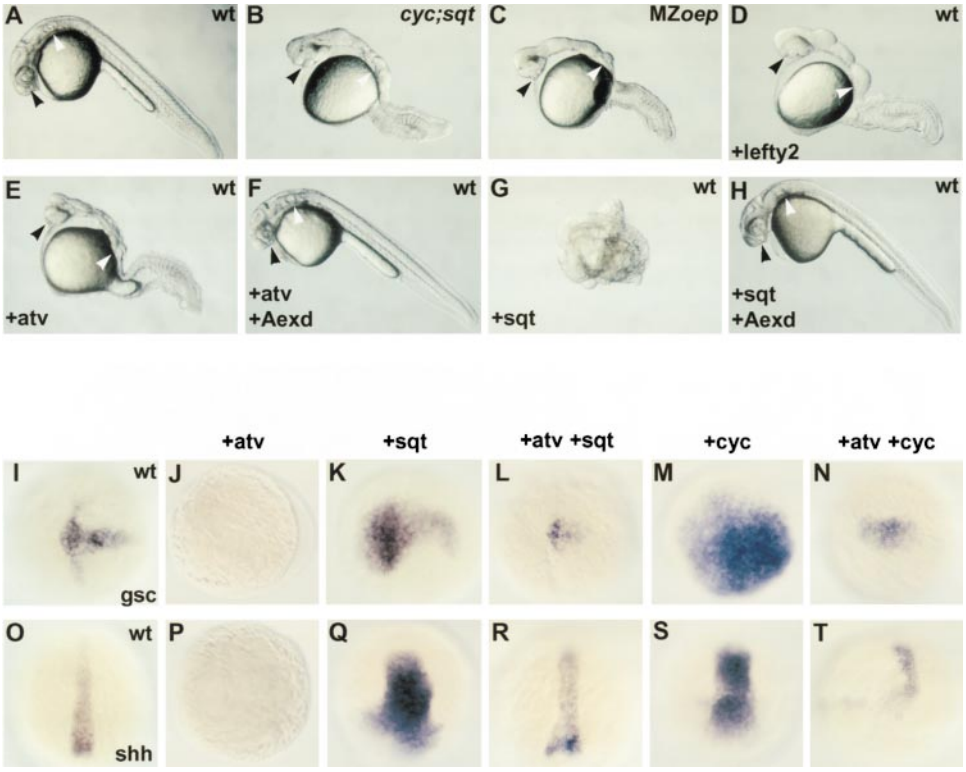

Figure 5. Mouse Lefty2 and Zebrafish Antivin Antagonize Nodal Signaling in Zebrafish

(A–H) Live zebrafish embryos at 30 hr postfertilization. (A–F, H) Black arrowheads indicate the eyes, and white arrowheads highlight the otic vesicle. (A) Wild-type embryo. (B) *cyclops;squint* double-mutant embryo. (C) Maternal zygotic *oep* (MZ*oep*) mutant embryo. (D–H) Wild-type embryos were injected with 5 pg of *lefty2* RNA (D; 152/153 had the phenotype shown), 5 pg of *antivin* (*atv*) RNA ([E] 39/51), 5 pg *atv* RNA + 250 pg *Aexd* RNA encoding the extracellular domain of ActRIIB ([F] 70/70 were rescued, and 53 of those had the phenotype shown), 10 pg of *squint* (*sqt*) RNA ([G] 27/27 were severely dorsalized), or 10 pg of *sqt* RNA + 250 pg of *Aexd* RNA ([H] 15/27 were rescued, and 4 of those had the phenotype shown). (I–T) Wild-type embryos at 90% epiboly (10 hr). (I–N) *Goosecoid (gsc)* RNA expression is shown in uninjected embryos (I) or in embryos injected with 5 pg of *atv* RNA ([J] 35/36 did not express *gsc*), 10 pg of *sqt* RNA ([K] 23/27 expressed *gsc* ectopically), 5 pg of *atv* RNA + 10 pg of *sqt* RNA ([L] 9/30 expressed *gsc*), 10 pg of *cyc* RNA (M; 27/27 expressed *gsc* ectopically), and 5 pg of *atv* RNA + 10 pg of *cyc* RNA ([N] 12/24 expressed *gsc*). (O–T) *Sonic hedgehog (shh)* expression is shown in uninjected embryos (O) or in embryos injected with 5 pg of *atv* RNA ([P] 18/21 did not express *shh*), 10 pg of *sqt* RNA ([Q] 31/32 expressed *shh* ectopically), 5 pg of *atv* RNA + 10 pg of *sqt* RNA ([R] 18/24 expressed *shh*), 10 pg of *cyc* RNA ([S] 25/34 expressed *shh* ectopically), and 5 pg of *atv* RNA + 10 pg of *cyc* RNA ([T] 20/20 expressed *shh*).

data not shown). These results suggest that Lefty2 and Antivin overexpression initially blocks Nodal signaling and then blocks *sqt* and *cyc* transcription secondarily, by interfering with *nodal* autoregulation.

The Lack of *lefty2* Results in Upregulation of *nodal*

The results in zebrafish suggested that Antivin/Lefty2 block Nodal signaling, which in turn leads to a block of *nodal* transcription. These observations predict that *nodal* transcription is initially normal and subsequently expanded in *lefty2* mutants. We tested this hypothesis by analyzing the expression of *nodal* in *lefty2* mutants (Figure 7). Since the *nodal* mutant allele utilized in the current studies was generated by the introduction of an *IRES-lacZ* reporter sequence (Collignon et al., 1996), we first monitored the expression of *nodal* in *lefty2* mutants by staining embryos with X-gal. *LacZ* expression in *lefty2*$^{-/-}$ *nodal*$^{lacZ/+}$ embryos was not affected between E6.5 and E7.25 (Figure 7D), consistent with our hypothesis and the previous observation that *lefty2* expression begins at E6.5 (Figure 1C), much later than the onset of *nodal* expression (Varlet et al., 1997a). Intriguingly, however, *lefty2*$^{-/-}$ *nodal*$^{lacZ/+}$ mutant embryos at E8.0 showed very intense X-gal staining in the ectoderm that extended laterally and anteriorly (Figure 7E). Transverse sections confirmed the upregulation and lateral expansion of *lacZ* expression domain in the ectoderm and visceral endoderm (Figure 7F). In contrast, X-gal staining was restricted to the node of *lefty2*$^{+/+}$ *nodal*$^{lacZ/+}$ embryos at E8.0 (Figure 7B). A weak level of staining was also seen in posterior ectoderm at E8.0 (Figures 7B and 7C), as previously reported (Collignon et al., 1996; Varlet et al., 1997a). As the *lefty2*$^{-/-}$ *nodal*$^{lacZ/+}$ embryos have a milder phenotype than *lefty2*$^{-/-}$ *nodal*$^{+/+}$ embryos, we also examined *nodal* expression by whole-mount in situ hybridization in *lefty2*$^{-/-}$ *nodal*$^{+/+}$ embryos. In wild-type embryos, *nodal* mRNA was localized to the posterior epiblast and endoderm at E7.0 (Figure 7G) but was restricted to the node at E7.5 (Figures 7H and 7I). In *lefty2*$^{-/-}$ *nodal*$^{+/+}$ embryos, *nodal* mRNA distribution remained normal until E7.0 (Figure 7J). However, at E7.5,

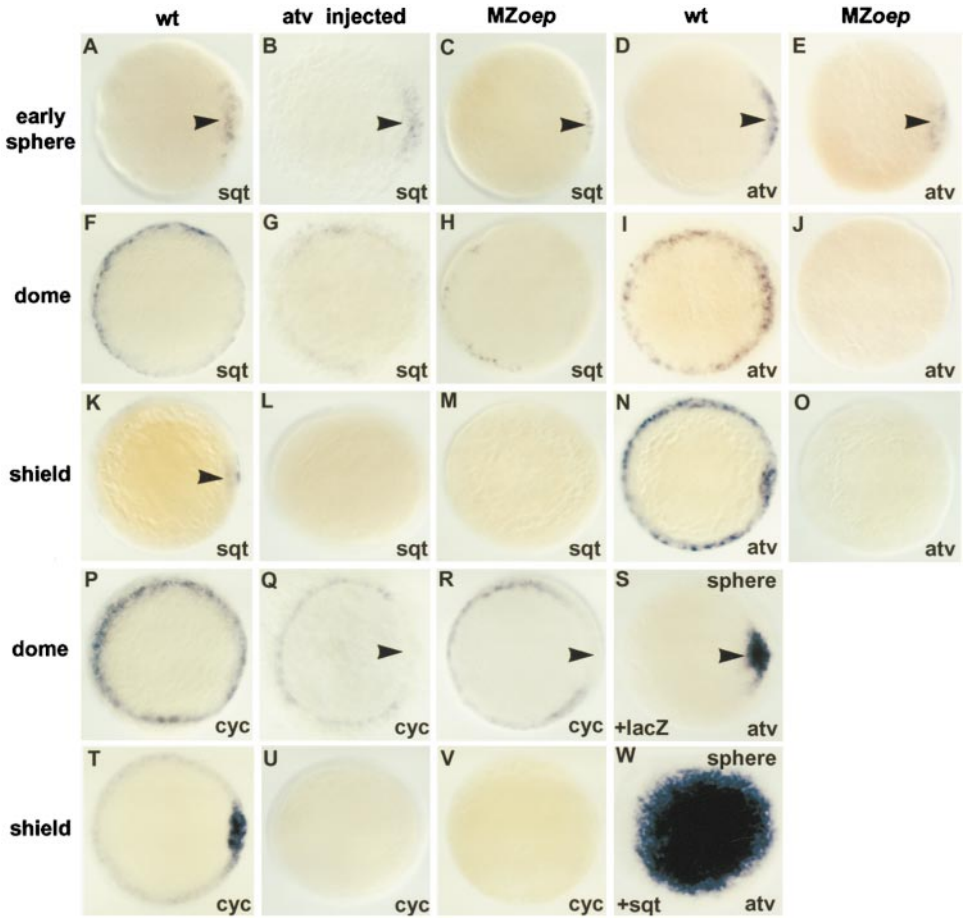

Figure 6. Expression of *antivin*, *cyclops*, and *squint* Is Dependent on Nodal Signaling

Expression of *sqt* RNA (A–C, F–H, K–M), *cyc* RNA (P–R, T–V), and *atv* RNA (D, E, I, J, N, O, S, W) in zebrafish embryos. The black arrowhead in (K) indicates dorsal *sqt* expression in the shield. (A–E, S, W) Early sphere stage (4 hr). Black arrowheads indicate dorsal expression of *sqt* (A–C) and *atv* (D–E, S). (F–J, P–R) Dome stage (5.5 hr). (K–O, T–V) Shield stage (7.2 hr). (A, B, D, F, G, I, K, L, N, P, Q, S–U, W) Wild-type embryos. (C, E, H, J, M, O, R, V) MZ*oep* mutant embryos. Note that *atv* is expressed at early sphere stage (E), but not at dome stage (J) or shield stage (O) in MZ*oep* mutants. (A, C–F, H–K, M–P, R, T, V) Uninjected embryos. (B, G, L, Q, U) Embryos injected with 10 pg of *atv* RNA. Note that *sqt* is expressed at sphere stage ([B] 8 out of 11 embryos) and dome stage ([G] 13/15), but not at shield stage ([L] 15/15) in *atv*=injected embryos. This parallels *sqt* expression in MZ*oep* mutants (compare [B] with [C], [G] with [H], and [L] with [M]). Note that *cyc* is expressed at dome stage ([Q] 13/16) but not at shield stage ([U] 13/15) in *atv*-injected embryos. This parallels *cyc* expression in MZ*oep* mutants (compare [Q] with [R], and [U] with [V]). The arrowheads in (Q) and (R) highlight the gap of cyc expression on the dorsal side in *atv*-injected embryos (Q) and in MZ*oep* mutants (R). (S) Embryos injected with 10 pg of *lacZ* RNA. Note that *atv* expression is unaffected in *lacZ* RNA injected controls (13/13). (W) Embryos injected with 10 pg of *sqt* RNA. Note ectopic *atv* expression in *sqt*-injected embryos (13/13).

nodal expression was markedly upregulated in the visceral endoderm and the posterior/lateral ectoderm (Figures 7K and 7L). The finding that Lefty2 affects *nodal* transcription only after the induction of *nodal* expression suggests that loss of *lefty2* leads to augmentation of Nodal signaling, which in turn leads to enhanced *nodal* expression. Conversely, we also analyzed the expression of *lefty2* in *nodal* mutants. No *lefty2* expression was detected in *nodal*$^{-/-}$ embryos, likely reflecting the absence of mesoderm in *nodal* mutants (Figure 7N).

Discussion

Lefty2 and Antivin Block Nodal Signaling

Five lines of evidence establish that Lefty2 and Antivin act as antagonists of the Nodal signaling pathway. First, *lefty2* mutants have an expanded primitive streak, a phenotype opposite to that of *nodal* mutant embryos (Conlon et al., 1994). Second, the *lefty2* mutant phenotype is suppressed by heterozygosity for *nodal*, indicating that Lefty2 and Nodal act antagonistically. Third, *lefty2; nodal* double mutants have the same phenotype as *nodal* single mutants, demonstrating that the phenotypic defects in *lefty2* mutants are dependent on Nodal signaling. Fourth, overexpression of Lefty2 and Antivin induces defects identical to the phenotypes caused by the absence of the zebrafish Nodal signaling components *cyc* and *sqt* or *oep* (Feldman et al., 1998; Gritsman et al., 1999; Thisse and Thisse, 1999). Fifth, the effects of Antivin and Lefty2 can be overcome by overexpression of Cyc or Sqt. Thus, our results in mouse and zebrafish indicate that the primary role of Lefty2/Antivin is to attenuate Nodal signaling during gastrulation.

How do Lefty2 and Antivin block Nodal signaling? Two possibilities are that the extracellular antagonists Lefty/Antivin inactivate the signaling ligand Nodal, or block binding and activation of Nodal receptors (Piccolo et al., 1996; Zimmerman et al., 1996; Perrimon and McMahon,

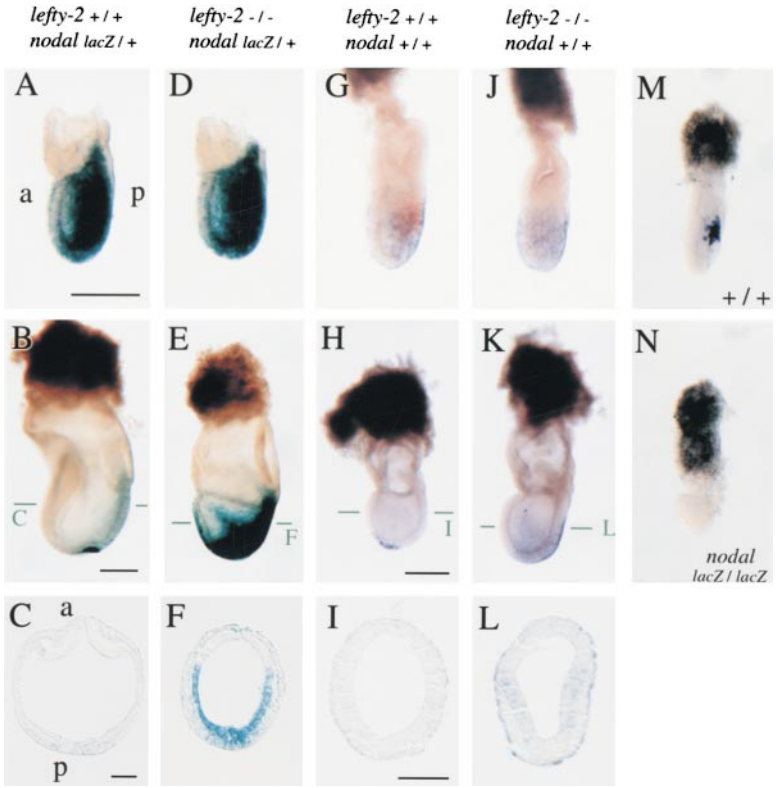

Figure 7. Lack of *lefty2* Results in Upregulation of *nodal*

(A–F) *lefty2*$^{+/+}$ *nodal*$^{lacZ/+}$ (A–C) and *lefty2*$^{-/-}$ *nodal*$^{lacZ/+}$ (D–F) embryos were recovered at E7.25 (A and D) or E8.0 (B, C, E, and F), and the expression of *nodal* was monitored by X-gal staining. (C) and (F) are transverse sections of the embryos shown in (B) and (E), respectively. In the *lefty2*$^{+/+}$*nodal*$^{lacZ/+}$ embryo, X-gal staining was apparent in the posterior epiblast at E7.25 (A) but was confined to the node at E8.0 (B), as described previously (Collignon et al., 1996). In the *lefty2*$^{-/-}$ *nodal*$^{lacZ/+}$ embryo, X-gal staining is normal at E7.25 (D). However, the staining is markedly upregulated and expanded at E8.0 ([E] and [F]; the intense staining was seen in the posterior and lateral ectoderm and mesoderm). (G–L) *nodal* expression in the wild-type (G–I) and *lefty2*$^{-/-}$ *nodal*$^{+/+}$ (J–L) embryos was examined by in situ hybridization at E7.0 (G and J) or E7.5 (H and K). (I) and (L) are transverse sections of the embryos shown in (H) and (K), respectively. Two-color in situ hybridization was performed in (G) and (J); *nodal* transcript in blue, and *lefty2* transcript in red. At E7.5, *nodal* expression was confined to the node in the wild-type embryo (H and I) while, in *lefty2*$^{-/-}$ *nodal*$^{+/+}$ embryos, intense expression was observed in a much wider area including the endoderm and ectoderm (K and L). Expansion of *nodal* expression in the epiblast might lead to the paracrine induction of *nodal* in the visceral endoderm by autoregulation. Scale bars in the top, middle, and bottom panels represent 250 μm, 250 μm, and 100 μm, respectively.

(M and N) *lefty2* expression in the wild-type (M) and *nodal*$^{lacZ/lacZ}$ (N) embryos at E6.5. *lefty2* expression is abolished in the *nodal*$^{lacZ/lacZ}$ embryo (N).

1999). The first possibility is less likely because structural considerations suggest that Lefty2 and Antivin, unlike typical TGFβ family members, are unable to form heterodimers (Thisse and Thisse, 1999). Genetic analyses suggest that extracellular components of the Nodal signaling pathway include EGF-CFC proteins (Gritsman et al., 1999), ActRIB (Gu et al., 1998; Gritsman et al., 1999), and ActRIIB (Oh and Li, 1997; Figure 5) or related receptors. Activated forms of type I receptors such as ActRIB or TARAM-A mimic activation of Nodal signaling in zebrafish (Gritsman et al., 1999) and suppress the effects of *antivin* overexpression (Thisse and Thisse, 1999). Furthermore, coexpression of the ActRIIB ectodomain blocks both Squint and Antivin (Figure 5). These results support the idea that Antivin and Lefty2 bind to Nodal receptors, thereby inhibiting binding of Nodal signals or blocking the activation of the receptors. While these results suggest that Lefty2 and Antivin could also block signaling by activin or other TGFβ signals, our in vivo results indicate a relatively specific interaction with Nodal signaling during early embryogenesis.

Positive and Negative Feedback Loops Regulate the Expression of *nodal/cyc/sqt* and *lefty2/antivin*

The transcription of *lefty2/antivin* and *nodal/cyc/sqt* appears to be regulated by a positive and a negative feedback mechanism. A positive feedback loop wherein Nodal signaling maintains and enhances *nodal* transcription is evidenced by two observations. First, maintenance, but not induction, of *cyc* and *sqt* expression is dependent on Nodal signaling. Second, the increase in Nodal signaling in *lefty2* mutants augments *nodal* transcription. Two observations suggest a negative feedback loop wherein Nodal signals induce their antagonists. First, ectopic activation of Nodal signaling induces *antivin* expression. Second, induction of *antivin* expression in the lateral and ventral margin and maintenance on the dorsal side are dependent on active Nodal signaling.

Based on these results, we propose the following time course for Nodal signaling and its regulation by Antivin and Lefty2 during mesoderm formation. First, transcription of *nodal*, *cyc*, and *sqt* is initiated by upstream factors that are independent of Nodal signaling. This leads to the activation of the Nodal signaling pathway, which maintains *sqt* and *cyc* transcription in a positive feedback loop but also initiates *antivin* and *lefty2* expression in most of the prospective mesoderm. Expression of Antivin and Lefty2 proteins activates a negative feedback loop to inhibit Nodal signaling, possibly by blocking ActRIIB and other potential Nodal receptors. This in turn leads to a reduction in *cyc* and *sqt* expression, resulting in the further attenuation of Nodal signaling.

Together with the agonistic and antagonistic activities of Nodal signals and Lefty2/Antivin, respectively, this model suggests that the balance of *lefty2/antivin* expression versus *nodal/cyc/sqt* expression controls the range and duration of Nodal signaling and the extent of mesoderm formation in zebrafish and mouse. In *lefty2* mutants, this balance would be disturbed, leading to an initial increase in Nodal signaling, which in turn leads to

augmented *nodal* transcription and further amplification of Nodal signaling. In this case, the absence of the negative feedback loop mediated by Lefty2 leads to overactivation of the positive feedback loop mediated by Nodal. Analogously, overexpression of Antivin or Lefty2 in zebrafish would mimic the overactivation of the negative feedback loop, resulting in the block of the positive feedback loop and loss of Nodal signaling and *cyc* and *sqt* expression. It is interesting to note that the relationship between *lefty2/antivin* and *nodal/cyc/sqt* is strikingly similar to that between *argos* and *spitz* in *Drosophila*. These secreted molecules act in a negative feedback loop as extracellular antagonist and agonist, respectively, of EGF receptor signaling (reviewed in Schweitzer and Shilo, 1997; Perrimon and McMahon, 1999).

Roles of Lefty Molecules in Left–Right Determination

Nodal signals and members of the Lefty family are expressed in the same or nearby domains not only during gastrulation but also at later stages of embryogenesis. For instance, *nodal/cyc* and *lefty2/antivin* are expressed asymmetrically in the left lateral plate during early somite stages (Collignon et al., 1996; Lowe et al., 1996; Meno et al., 1996, 1997; Varlet et al., 1997b; Rebagliati et al., 1998b; Thisse and Thisse, 1999). Based on the interaction during gastrulation and the remarkable relationship between *nodal/cyc* and *lefty/antivin* expression, we propose that Lefty proteins inhibit Nodal signaling in the lateral plate by interfering with the positive feedback loop that maintains *nodal* transcription. This extension of our feedback inhibition model to left–right determination would explain several recent observations. First, the asymmetric expression of *nodal* and *lefty2* has a very narrow time window (2–6 somite stage; Collignon et al., 1996; Lowe et al., 1996; Meno et al., 1997), possibly reflecting the attenuation of Nodal signaling and *nodal* expression by Lefty2. Second, *nodal* and *lefty2* transcription in the left lateral plate is controlled by similar left side–specific *cis*-acting elements (Adachi et al., 1999; Norris and Robertson, 1999; Saijoh et al., 1999). Our model suggests that both enhancers might be activated by Nodal signaling. Third, in *lefty1* mutants, *nodal* and *lefty2* are ectopically expressed on the right side (Meno et al., 1998; Adachi et al., 1999). We previously proposed that Lefty1 protein in the prospective floor plate blocks expression of *nodal* and *lefty2* in the right lateral plate by blocking a postulated signal X. The findings presented here indicate that Lefty1 normally blocks a Nodal signal, supporting the possibility that factor X (Meno et al., 1998) is in fact Nodal. The absence of Lefty1 would relieve this block and activate *nodal* and *lefty2* ectopically (Meno et al., 1998).

In summary, the results reported here suggest that an evolutionarily conserved antagonism between Lefty proteins and Nodal signals fine tunes developmental processes ranging from mesoderm formation to left–right axis determination. The dependence of Nodal signaling on EGF-CFC proteins (Gritsman et al., 1999) and the attenuation of Nodal signaling by feedback inhibitors of the Lefty family provide a sophisticated extracellular control of Nodal-mediated inductive processes during vertebrate embryogenesis.

Experimental Procedures

Generation of *lefty2*-Deficient Mice

Genomic *lefty2* clones were isolated from a genomic library constructed from E14 ES cells. To construct a targeting vector, the 5′-flanking region (the SalI-SacI 3 kb fragment), a STneo cassette from pSTneo (the SacI-XbaI fragment), and the 3′-flanking region (the XbaI-SalI 9 kb fragment) were subcloned in Bluescript. Targeting was performed as described previously (Sawai et al., 1991). The targeting vector was linearized with NotI before electroporation into E14 ES cells. Of 75 G418-resistant ES clones, 11 (15%) were found to have undergone homologous recombination, which was confirmed by Southern blot analysis with various probes such as a 5′-flanking probe (Figure 1A), 3′-flanking probe, and a *neo* probe. Two targeted ES cell lines were separately injected into blastocysts obtained from the mating between C57BL/6Cr and F1 [C57BL/6Cr × C3H], resulting in the birth of chimeric mice. Male chimeras derived from each ES cell line were bred to C57BL/6Cr, resulting in heterozygous F1 offsprings. The heterozygotes were mated with each other, producing *lefty2*$^{-/-}$ embryos. The two targeted ES cell lines produced *lefty2*$^{-/-}$ homozygotes showing indistinguishable phenotypes. All analyses were carried out on a mixed B6/129 background.

In Situ Hybridization and Histology

Mouse embryos were staged based on their morphology and the number of the somites. For histology, embryos were fixed with Bouin's solution, embedded into paraffin, and sectioned at 7 μm thickness. Sections in Figure 2 and Figure 4B were stained with hematoxylin and eosine. Whole-mount in situ hybridization followed standard protocols (Wilkinson, 1992). Embryos were genotyped by PCR of yolk sac DNA with the following primers: 5′-GCCTGACCTAGAGTCG TTTC and 5′-GGAAGAGCTCACCTCGAAAA for the wild-type *lefty2* allele, and 5′-GCCTGACCTAGAGTCGTTTC and 5′-ACCCAGCACTC CACTGGATA for the mutant *lefty2* allele. Probes specific to *lefty1* and *lefty2* do not cross-hybridize to each other since they are derived from the 3′-untranslated regions (Meno et al., 1997). INT/BCIP solution (Boehringer Mannheim) was used as a red substrate for in situ hybridization with X-gal-stained embryos (Figure 1O) and for two-color whole-mount in situ hybridization (Figures 7G and 7J).

Analysis of Genetic Interaction between *lefty2* and *nodal*

nodal mutant mice, in which an *IRES-LacZ* cassette is inserted into the second exon of the *nodal* gene, have been described previously (Collignon et al., 1996). *Nodal*$^{lacZ/+}$ mice were crossed with *lefty2*$^{+/-}$ mice to obtain double heterozygotes. Embryos obtained by intercrossing the double heterozygotes or by crossing double heterozygotes with *lefty2*$^{+/-}$ animals were analyzed. The genotype of each embryo was determined by PCR. *nodal* expression in these embryos was monitored by staining with X-gal.

Zebrafish Strains

Wild-type embryos were obtained from intercrosses between fish from the Tuebingen Longfin (TL) inbred strain. Maternal-zygotic *oep*^{tz57} (MZ*oep*) mutant embryos were obtained as described in Gritsman et al. (1999). To obtain *sqt;cyc* double-mutant embryos, fish with the genotype *sqt*$^{ny1/+}$; *cycm*$^{294/+}$ were intercrossed, as described in Feldman et al. (1998).

Phenotypic Analysis

Zebrafish embryos were staged according to Kimmel et al. (1995). Live embryos were analyzed and photographed on a Leica MZ APO dissecting microscope. In situ hybridization was performed as described (Zhang et al., 1998). *antivin* probe was transcribed from pBSK+antivin (NotI,T7; Thisse and Thisse, 1999). The *cyclops* probe was transcribed from pCyclops (NotI,T7; Rebagliati et al., 1998b).

RNA Microinjections

The following plasmids were linearized, and sense strand–capped mRNA was synthesized using the mMESSAGE mMACHINE system (Ambion): pSP64T-Xβ nodal (mouse *nodal*; EcoRI, SP6; Toyama et al., 1995), pCS2+cyclops (NotI, SP6; Rebagliati et al., 1998a), pCS2+squint (NotI, SP6; Feldman et al., 1998), pCS2+antivin (NotI,

SP6; Thisse and Thisse, 1999), pActRIIBexd/RN3P (extracellular domain of the activin type II receptor ActRIIB; SfiI, T3; Dyson and Gurdon, 1997), pCS2+lefty2 (NotI, SP6), and pCS2+lacZ (NotI, SP6). Injections were performed as described in Gritsman et al. (1999).

Acknowledgments

We thank R. Beddington, I. Dawid, S. Dougan, Y. Imai, G. Martin, B. Hermann, Y. Saga, H. Sasaki, S. Wilson, C. Wright, and B. and C. Thisse for sharing reagents used in this study; Y. Saijoh for his comments; and K. Miyama and T. Tanabe for their excellent technical assistance. This work was supported by grants from the Ministry of Education, Science, Sports, and Culture of Japan (to H. H. and H. K.), by a grant from CREST (Core Research for Evolutional Science and Technology) of Japan Science and Technology Corporation (to H. H.), and by grants from NIH (to A. F. S., W. S. T, and E. J. R.).

Received April 28, 1999; revised June 14, 1999.

References

Adachi, H., Saijoh, Y., Mochida, K., Ohishi, S., Hashiguchi, H., Hirao, A., and Hamada, H. (1999). Determination of left-right asymmetric expression of *nodal* by a left side-specific enhancer with sequence similarity to a *lefty2* enhancer. Genes Dev., *13*, 1589–1600.

Ang, S.-L., Conlon, R.A., Jin, O., and Rossant, J. (1994). Positive and negative signals from mesoderm regulates the expression of mouse *Otx2* in ectoderm explants. Development *120*, 2979–2989.

Beddington, R., and Robertson, E.J. (1999). Axis development and early asymmetry in mammals. Cell *96*, 195–209.

Candia, A.F., Hu, J., Crosby, J., Lalley, P.A., Noden, D., Nadeau, J.H., and Wright, C.V.E. (1992). Mox-1 and Mox-2 define a novel homeobox gene subfamily and are differentially expressed during early mesodermal patterning in mouse embryos. Development *116*, 1123–1136.

Collignon, J., Varlet, I., and Robertson, E.J. (1996). Relationship between asymmetric *nodal* expression and the direction of embryonic turning. Nature *381*, 155–158.

Conlon, F.L., Lyons, K.M., Takaesu, N., Barth, K.S., Kispert, A.K., Herrmann, B., and Robertson, E.J. (1994). A primary requirement of *nodal* in the formation and maintenance of the primitive streak in mouse. Development *120*, 1919–1928.

Crossley, P.H., and Martin, G.R. (1995). The mouse *Fgf8* gene encodes a family of polypeptide and is expressed in regions that direct outgrowth and patterning in the developing embryo. Development *121*, 439–451.

Dyson, S., and Gurdon, J.B. (1997). Activin signaling has a necessary function in *Xenopus* early development. Curr. Biol. *7*, 81–84.

Feldman, B., Gates, M.A., Egan, E.S., Dougan, S.T., Renneback, G., Sirotkin, H.I., Schier, A.F., and Talbot, W.S. (1998). Zebrafish organizer development and germ-layer formation require nodal-related signals. Nature *395*, 181–185.

Gritsman, K., Zhang, J., Cheng, S., Heckscher, E., Talbot, W.S., and Schier, A.F. (1999). The EGF-CFC protein one-eyed pinhead is essential for Nodal signaling. Cell *97*, 121–132.

Gu, Z., Nomura, M., Simpson, B.B., Lei, H., Feijen, A., van den Eijnden-vanRaaij, J., Donahoe, P.K., and Li, E. (1998). The type I activin receptor ActRIB required for egg cylinder organization and gastrulation in the mouse. Genes Dev. *12*, 844–857.

Harland, R., and Gerhart, J. (1997). Formation and function of Spemann's organizer. Annu. Rev. Cell. Dev. Biol. *13*, 611–667.

Hatta, K., Kimmel, C.B., Ho, R.K., and Walker, C. (1991). The *cyclops* mutation blocks specification of the floor plate of the zebrafish central nervous system. Nature *350*, 339–341.

Kimmel, C.B., Ballard, W.W., Kimmel, S.R., Ullmann, B., and Schilling, T.F. (1995). Stages of embryonic development of the zebrafish. Developmental Dynamics *203*, 253–310.

Kispert, A., and Herrmann, B.G. (1994). Immunohistochemical analysis of the Brachyury protein in wild-type and mutant mouse embryos. Dev. Biol. *161*, 179–193.

Logan, M., Pagan-Westphal, S.M., Smith, D.M., Paganessi, L., and Tabin, C. (1998). The transcription factor Pitx2 mediates situs-specific morphogenesis in response to left–right asymmetric signals. Cell *94*, 307–318.

Lowe, L., Supp, D.M., Sampath, K., Yokoyama, T., Wright, C.V.E., Potter, S.S., Overbeek, P., and Kuehn, M.R. (1996). Conserved left-right asymmetry of *nodal* expression and alteration in murine *situs inversus*. Nature *381*, 158–161.

Massague, J. (1998). TGFβ signal transduction. Annu. Rev. Biochem. *67*, 753–791.

Meno, C., Saijoh, Y., Fujii, H., Ikeda, M., Yokoyama, T., Yokoyama, M., Toyoda, Y., and Hamada, H. (1996). Left-right asymmetric expression of the TGFβ-family member *lefty* in mouse embryos. Nature *381*, 151–155.

Meno, C., Itoh, Y., Saijoh, Y., Matsuda, Y., Tashiro, K., Kuhara, S., and Hamada, H. (1997). Two closely-related left-right asymmetrically expressed genes, *lefty1* and *lefty2*: their distinct expression domains, chromosomal linkage and direct neuralizing activity in *Xenopus* embryos. Genes Cells *2*, 513–524.

Meno, C., Shimono, A., Saijoh, Y., Yashiro, K., Ohishi, S., Mochida, K., Noji, S., Kondoh, H., and Hamada, H. (1998). *lefty1* is required for left-right determination as a regulator of *lefty2* and *nodal*. Cell *94*, 287–298.

Norris, D.P., and Robertson, E.J. (1999). Asymmetric and node-specific *nodal* expression patterns are controlled by two distinct cis-acting regulatory elements. Genes Dev. *13*, 1575–1588.

Oh, S.P., and Li, E. (1997). The signaling pathway mediated by the type IIB activin receptor controls axial patterning and lateral asymmetry in the mouse. Genes Dev. *11*, 1812–1826.

Oulad-Abdelghani, M., Chazaud, C., Bouillet, P., Mattei, M.G., Dolle, P., and Chambon, P. (1998). *Stra3/lefty*, a retinoic acid-inducible novel member of the TGFβ superfamily. Int. J. Dev. Biol. *42*, 23–32.

Perrimon, N., and McMahon, A.P. (1999). Negative feedback mechanisms and their roles during pattern formation. Cell *97*, 13–16.

Piccolo, S., Sasai, Y., Lu, B., and DeRobertis, E.M. (1996). Dorsoventral patterning in *Xenopus*: inhibition of ventral signals by direct binding of chordin to BMP-4. Cell *86*, 589–598.

Piedra, M.E., Icardo, J.M., Albajar, M., Rodriguez-Rey, J.C., and Ros, M.A. (1998). Pitx2 participates in the late phase of the pathway controlling left-right asymmetry. Cell *94*, 319–324.

Rebagliati, M.R., Toyama, R., Haffter, P., and Dawid, I.B. (1998a). *cyclops* encodes a nodal-related factor involved in midline signaling. Proc. Natl. Acad. Sci. USA *95*, 9932–9937.

Rebagliati, M.R., Toyama, R., Fricke, C., Haffter, P., and Dawid, I.B. (1998b). Zebrafish nodal-related genes are implicated in axial patterning and establishing left-right asymmetry. Dev. Biol. *199*, 261–272.

Ryan, A.K., Blumberg, B., Rodriguez-Estaban, C., Yonei-Tamura, S., Tamura, K., Tsukui, T., de la Pena, J., Sabbagh, W., Greenwald, J., Choe, S., et al. (1998). Pitx2 determines left-right asymmetry of internal organs in vertebrates. Nature *394*, 545–551.

Saijoh, Y., Adachi, H., Hirao, A., Mochida, K., Ohishi, S., and Hamada, H. (1999). Distinct transcriptional regulatory mechanisms underlie left-right asymmetric expression of *lefty1* and *lefty2*. Genes Dev. *13*, 259–269.

Sampath, K., Rubinstein, A.L., Cheng, A.M., Liang, J.O., Fekany, K., Solnica-Krezel, L., Korzh, V., Halpern, M.E., and Wright, C.V.E. (1998). Induction of the zebrafish ventral brain and floor plate requires cyclops/nodal signaling. Nature *395*, 185–189.

Sasaki, H., and Hogan, B.L.M. (1993). Differential expression of multiple fork head related genes during gastrulation and axial pattern formation in the mouse embryo. Development *118*, 47–59.

Sawai, S., Shimono, A., Hanaoka, K., and Kondoh, H. (1991). Embryonic lethality resulting from disruption of both *N-myc* alleles in mouse zygotes. New Biologists *9*, 861–869.

Schweitzer, R., and Shilo, B.Z. (1997). A thousand and one roles for the *Drosophila* EGF receptor. Trends Genet. *13*, 191–196.

Thisse, C., and Thisse, B. (1999). Antivin, a novel and divergent member of the TGFβ superfamily, negatively regulates mesoderm induction. Development *126*, 229–240.

Thomas, P., and Beddington, R. (1996). Anterior primitive endoderm may be responsible for patterning the anterior neural plate in the mouse embryo. Curr. Biol. *6*, 1487–1496.

Toyama, R., O'Connell, M.L., Wright, C.V., Kuehn, M.R., and Dawid, I.B. (1995). Nodal induces ectopic goosecoid and lim1 expression and axis duplication in zebrafish. Development *121*, 383–391.

Varlet, I., Collignon, J., and Robertson, E.J. (1997a). Nodal expression in the primitive eododerm is required for the specification of the anterior axis during mouse gastrulation. Development *124*, 1033–1044.

Varlet, I., Collignon, J., Norris, D.P., and Robertson, E.J. (1997b). Nodal signaling and axis formation in the mouse. Cold Spring Harb. Symp. Quant. Biol. *62*, 105–113.

Wolf, C., Thisse, C., Stoetzel, C., Thisse, B., Gerlinger, P., and Perrin-Schmitt, F. (1991). The *M-twist* gene of *Mus* is expressed in subsets of mesodermal cells and is closely related to the *Xenopus X-twi* and the *Drosophila twist* genes. Dev. Biol. *143*, 363–373.

Wilkinson, D.G. Whole mount in situ hybridization of vertebrate embryos. In In Situ Hybridization: A Practical Approach, D.G. Wilkinson, ed. (IRL Press, Oxford 1992), 75–84.

Yoshioka, H., Meno, C., Koshiba, K., Sugihara, M., Itoh, H., Ishimaru, Y., Inoue, T., Ohuchi, H., Semina, E.V., Murray, J.C., et al. (1998). *Pitx2*, a bicoid type homeobox gene, is involved in a Lefty-signaling pathway in determination of left-right asymmetry. Cell *94*, 299–305.

Zhang, J., Talbot, W.S., and Schier, A.F. (1998). Positional cloning identifies zebrafish one-eyed pinhead as a permissive EGF-related ligand required for gastrulation. Cell *92*, 241–251.

Zimmerman, L.B., De Jesus-Escobar, J.M., and Harland, R.M. (1996). The Spemann organizer signal noggin binds and inactivates bone morphogenetic protein 4. Cell *86*, 599–606.

Zhou, X., Sasaki, H., Lowe, L., Hogan, B.L., and Kuehn, M.R. (1993). Nodal is a novel TGFβ-like gene expressed in the mouse node during gastrulation. Nature *361*, 543–547.